Title

Rehabilitative Training Interacts with Ischemia-Instigated Spine Dynamics to Promote a Lasting Population of New Synapses in Peri-Infarct Motor Cortex

Journal

Journal of Neuroscience, 39(43)

ISSN

0270-6474

Authors

Clark, Taylor A
Sullender, Colin
Jacob, Daron
et al.

Publication Date

2019-10-23

DOI

10.1523/jneurosci.1141-19.2019

Peer reviewed

Development/Plasticity/Repair

Rehabilitative Training Interacts with Ischemia-Instigated Spine Dynamics to Promote a Lasting Population of New Synapses in Peri-Infarct Motor Cortex

Taylor A. Clark,[1] Colin Sullender,[2] Daron Jacob,[3] Yi Zuo,[4] Andrew K. Dunn,[2] and Theresa A. Jones[1]

[1]Institute for Neuroscience, [2]Department of Biomedical Engineering, University of Texas at Austin, Austin, Texas 78712, [3]School of Medicine, Texas Tech Health Sciences Center, Lubbock, Texas 79430, and [4]Molecular, Cell, and Developmental Biology, University of California at Santa Cruz, Santa Cruz, California 95064

After subtotal infarcts of primary motor cortex (M1), motor rehabilitative training (RT) promotes improvements in paretic forelimb function that have been linked with its promotion of structural and functional reorganization of peri-infarct cortex, but how the reorganization unfolds is scantly understood. Cortical infarcts also instigate a prolonged period of dendritic spine turnover in peri-infarct cortex. Here we investigated the possibility that synaptic structural responses to RT in peri-infarct cortex reflect, in part, interactions with ischemia-instigated spine turnover. This was tested after artery-targeted photothrombotic M1 infarcts or Sham procedures in adult (4 months) C57BL/6 male and female GFP-M line ($n = 24$) and male yellow fluorescent protein-H line ($n = 5$) mice undergoing RT in skilled reaching or no-training control procedures. Regardless of training condition, spine turnover was increased out to 5 weeks postinfarct relative to Sham, as was the persistence of new spines formed within a week postinfarct. However, compared with no-training controls, new spines formed during postinfarct weeks 2–4 in mice undergoing RT persisted in much greater proportions to later time points, by a magnitude that predicted behavioral improvements in the RT group. These results indicate that RT interacts with ischemia-instigated spine turnover to promote preferential stabilization of newly formed spines, which is likely to yield a new population of mature synapses in peri-infarct cortex that could contribute to cortical functional reorganization and behavioral improvement. The findings newly implicate ischemia-instigated spine turnover as a mediator of cortical synaptic structural responses to RT and newly establish the experience dependency of new spine fates in the postischemic turnover context.

Key words: dendritic spines; *in vivo* imaging; ischemia; mouse models; photothrombosis; rehabilitative training

Significance Statement

Motor rehabilitation, the main treatment for motor impairments after stroke, is far from sufficient to normalize function. A better understanding of neural substrates of rehabilitation-induced behavioral improvements could be useful for understanding how to optimize it. Here, we investigated the nature and time course of synaptic responses to motor rehabilitative training *in vivo*. Focal ischemia instigated a period of synapse turnover in peri-infarct motor cortex of mice. Rehabilitative training increased the stability of new synapses formed during the initial weeks after the infarct, the magnitude of which was correlated with improvements in skilled motor performance. Therefore, the maintenance of new synapses formed after ischemia could represent a structural mechanism of rehabilitative training efficacy.

Introduction

Stroke instigates a prolonged period of neuroanatomical reorganization in brain regions that are adjacent and connected to the core region of damage (Jones and Adkins, 2015). Plasticity-related genes become upregulated, and regenerative reactions, such as axonal sprouting, dendritic remodeling, and synapse turnover, proceed for weeks to months (Cramer and Chopp, 2000; Carmichael, 2006; Brown et al., 2007). That many regenerative response are neural activity-dependent and sensitive to be-

Received May 16, 2019; revised Aug. 23, 2019; accepted Sept. 2, 2019.

Author contributions: T.A.C. and T.A.J. designed research; T.A.C. and C.S. performed research; T.A.C., C.S., and D.J. analyzed data; T.A.C. wrote the first draft of the paper; T.A.C., Y.Z., A.K.D., and T.A.J. edited the paper; T.A.C. and T.A.J. wrote the paper.

This work was supported by National Institutes of Health, National Institute of Neurological Disorders and Stroke NS078791 to T.A.J, A.K.D, and Y.Z. and NS101564 and NS056839 to T.A.J.

The authors declare no competing financial interests.

Correspondence should be addressed to Taylor A. Clark at clark.taylorann@utexas.edu.

https://doi.org/10.1523/JNEUROSCI.1141-19.2019

havioral experiences (Yu and Zuo, 2011; Allred et al., 2014; Jones, 2017; Tennant et al., 2017) should in theory create windows of opportunity during which behavioral manipulations could shape neural reorganization patterns in a manner that optimizes functional outcome. However, it is not presently clear what postischemic responses might be optimally targeted with behavioral manipulations, nor how exactly to target them. One strategy for beginning to fill this knowledge gap is to examine how neural remodeling responses are affected by behavioral manipulations that improve function in regions that mediate the functional improvements.

Following subtotal ischemic infarcts of primary motor cortex (M1) in rodents and primates, rehabilitative training (RT) of the paretic forelimb promotes maintenance and expansion of forelimb motor maps (Castro-Alamancos and Borrel, 1995; Nudo et al., 1996; Conner et al., 2005; Ramanathan et al., 2006) and, in rodents, increases dendritic complexity and synapse density and maturation (Wang et al., 2016; Kim et al., 2018) in residual motor cortex. Gain- and loss-of-function manipulations support that RT-driven behavioral improvements depend on the region of reorganization (Castro-Alamancos and Borrel, 1995; Dancause et al., 2005; Ramanathan et al., 2006; Nudo, 2007; Kim et al., 2018). However, little is known about the time course over which RT drives synaptic structural changes in remaining motor cortex, such that the temporal relation of these synaptic changes with behavioral improvements and whether they reflect interactions with ischemia-instigated remodeling responses have been unknown.

Monitoring synapses over time *in vivo* provides an opportunity to examine the influence of behavioral experiences on synaptic remodeling events as they unfold over time and their temporal relationships with behavioral change. Previous *in vivo* studies in mice have revealed that cortical ischemia increases dendritic spine turnover in peri-infarct cortex for weeks (Brown et al., 2007, 2010). New spines formed during the weeks following middle cerebral artery occlusion were more likely to remain over time compared with new spines formed in intact animals (Mostany and Portera-Cailliau, 2011). However, the possibility that postischemic patterns of spine turnover and new spine persistence are shaped by behavioral experiences had not been previously examined.

The primary goal of the present study was to determine whether RT impacts dendritic spine turnover responses to ischemia in peri-infarct motor cortex over time and, if so, whether this is related to RT-driven improvements in skilled use of the paretic forelimb. This was studied after focal M1 infarcts induced with artery-targeted photothrombosis, a variation of the photothrombotic infarct model, which increases the size of the vascular penumbra (Sullender et al., 2018; Clark et al., 2019), allowing us to examine spine dynamics in this expanded penumbra (Fig. 1). New spines formed during the initial postinfarct weeks were followed throughout the duration of RT to examine the relationship between new spine maintenance and behavioral recovery. Prior findings of increased densities of spines and synapses in peri-infarct cortex in response to RT were based on examinations deeper in cortex than the spines imaged *in vivo* (Wang et al., 2016; Kim et al., 2018), and patterns of spine change in response to motor skill training can vary between superficial and deeper apical dendrites of layer V pyramidal neurons (Clark et al., 2018). Thus, a second goal was to determine whether RT effects at the level of the superficial dendrites imaged *in vivo* are coupled with spine changes on deeper dendrites, as probed in endpoint measures of apical dendritic spine density in layers II/III of the same neuronal population imaged *in vivo*.

Materials and Methods

Experimental design. A description of the experimental design can be found in Figure 1.

Subjects. A total of 24 mice, including male ($n = 7$) and female ($n = 12$) C57BL/6 GFP-M line (B6/Cg-Tg (Thy-1 GFPM) 2Jrs/J; IMSR catalog #JAX:007788, RRID:IMSR_JAX:007788) and male ($n = 5$) C57BL/6 yellow fluorescent protein (YFP)-H line (B6/Cg-Tg (Thy-1 YFPH) 2Jrs/J; IMSR catalog #JAX:003782, RRID:IMSR_JAX:003782) were used. Both mouse lines express fluorescent proteins in a subset of layer 5 cortical pyramidal neurons, and both were included to probe generalization of results across them. All animals were bred at the Animal Resource Center at the University of Texas at Austin (ARC) and were between 4 and 5 months of age at the time of cranial window implantation. Estimations of sample sizes were based on group sizes from a previous study examining spine turnover in intact animals during motor skills training (Clark et al., 2018), as well as calculations of the minimum sample size needed to obtain a significant result with a power level of 0.8, from preliminary pilot data. Approximately equal numbers of male and female mice were randomly placed into 1 of 4 groups before any experimental procedures: (1) artery-targeted photothrombosis and rehabilitative training (infarct RT, $n = 3$ males, $n = 3$ females), (2) artery-targeted photothrombosis without rehabilitative training (infarct No RT, $n = 5$ males, $n = 5$ females), (3) Sham (no infarct) procedures and RT ($n = 3$ males, $n = 1$ female), or (4) Sham procedures and No RT ($n = 2$ males, $n = 3$ females). Two animals ($n = 1$ female infarct No RT, and $n = 1$ male Sham No RT) were included in behavioral analyses but not in spine dynamics analyses due to extremely dense YFP expression. One male and one female from the infarct No RT group were included in imaging analyses but excluded from behavioral analyses and correlations due to failure to perform the total number of trials on two of the testing days. Three animals (1 male infarct No RT, 1 female Sham No RT, and 1 female infarct RT) were excluded from the last imaging time point due to issues with window clarity. One animal with an overly small lesion was excluded for a failure to meet an *a priori* criterion for study inclusion that lesion volume be within 2 SDs of the group mean (female infarct No RT, not included in the group *n* above).

Mice were housed in a conventional vivarium in groups of 2–4 on a 12:12 h light/dark cycle. Lights were turned off between the hours of 6:00 P.M. and 6:00 A.M. daily, and temperature was maintained at 20°C. Each cage was supplied with wooden toys, bedding, and PVC pipes (cage enclosures; i.e., mice nest within them) that were replaced weekly. During behavioral procedures, mice were placed on scheduled feeding (2.5–3 g food once per day) to avoid satiation during behavioral training. Body weights were not permitted to fall to <90% of free feeding weights over the experimental time course (mean ± SE weight, 28.3 ± 1.2 g males and 21.3 ± 0.3 g females).

Animal use was in accordance with an Institutional Animal Care and Use Committee protocol (AUP-2015–00182) approved by the Animal Care and Use Committee of the University of Texas at Austin.

Cranial window creation. Cranial window implantation was performed as previously described (Clark et al., 2018). Briefly, mice were anesthetized with ketamine (4 mg/kg, i.p.) and xylazine (3 mg/kg, i.p.). Dexamethasone (2 mg/kg s.c.) and carprofen (2.5 mg/kg s.c.) were administered preoperatively to help minimize cortical swelling and inflammation during the procedures. Anesthetic plane was monitored via respiratory rate and toe pinch response throughout surgery. Booster injections of ketamine (4 mg/kg) were given as needed to maintain anesthesia. Following midline incision of the scalp, a 4 mm circular region of skull over frontoparietal cortex was thinned using a high-speed dental drill with a 0.5-mm-diameter drill bit and removed, leaving dura intact. Saline was frequently applied to protect the brain from overheating. Skull was then replaced with a 4-mm-diameter No. 1 coverglass (Warner, catalog #64–075) and sealed with cyanoacrylate (Vetbond, 3M) and dental cement. All windows were made over the forelimb area of M1 contralateral to the preferred-for-reaching forelimb (Fig. 1*B*). Following surgery, animals were given buprenorphine (100 mg/kg, s.c.) for pain

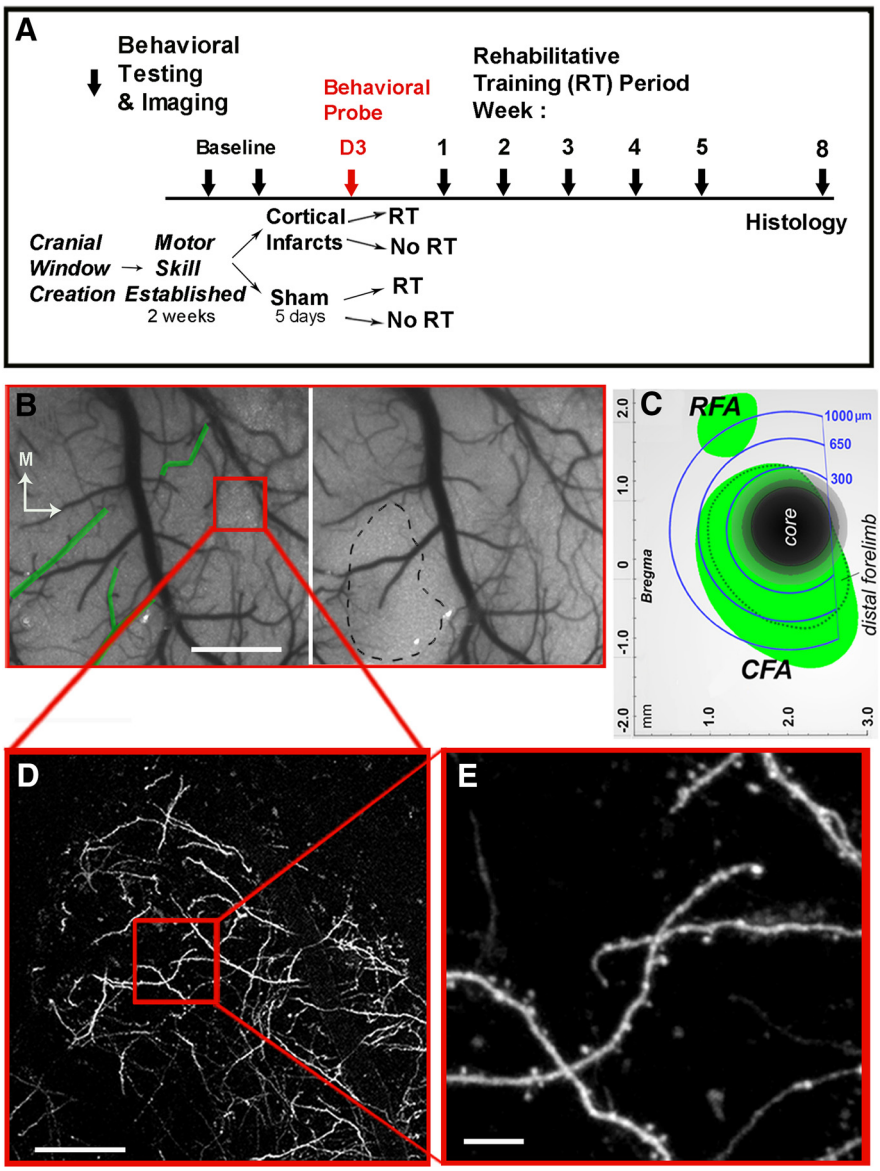

Figure 1. Experimental design. ***A***, Experimental time course. Block arrows indicate time points of imaging sessions and behavioral probes. ***B***, Speckle contrast image of cortical surface vasculature just before (left) and 10 min following (right) artery-targeted photothrombosis. Green outlines indicate targeted arterioles. Black dashed line indicates the infarct core, as defined by the region with < 20% baseline CBF 10 min after stroke onset. Red box represents a dendritic sample region. Scale bar, 1 mm. ***C***, Schematic diagram of imaging zones relative to the ischemic core and to caudal (CFA) and rostral (RFA) forelimb areas defined previously from intracortical microstimulation mapping (Tennant et al., 2011). ***D***, Low-magnification image of GFP-labeled dendrites in the sample imaging location. Scale bar, 100 μm. ***E***, High-magnification image of the sampling region. Scale bar, 10 μm.

management and allowed to recover in their cage for 1 week during which time they were given daily injections of carprofen (2.5 mg/kg, i.p.) to help minimize inflammation that contributes to window clouding.

Skilled forelimb training and assessment. The standard laboratory cage environment of mice provides limited opportunity for skilled forepaw use, conferring experimenter control over that experience and requiring that the skilled reaching task be established with training before infarcts so that the influence of infarcts and RT on the recovery of its performance can be determined. Before photothrombosis or Sham procedures, all mice were trained to criterion on the single-seed retrieval task (Farr and Whishaw, 2002). Mice learned to reach for a millet seed placed on a platform outside of a custom-made clear Plexiglas training chamber (20 cm tall, 15 cm deep, and 8.5 cm wide, measured from outside; 0.5 cm thick Plexiglas). There were 4-mm-wide vertical openings on the left and right sides of the chamber for mice to reach through with either the left or right paw. The platform (8.5 cm long, 4 cm wide, and 1.2 cm tall) contained one well that was at a diagonal distance of 7.3 mm away from the window edge closest to the chamber center (i.e., relative to the front chamber wall face, a 7 mm perpendicular distance from the window and 2 mm parallel distance from window edge; see Fig. 2*A*). During initial shaping, mice were allowed to reach for millet seeds outside of both openings with either limb. The preferred-for-reaching forelimb was defined as the first limb used to make five consecutive reach attempts. For the remainder of shaping (~2–3 d), mice were encouraged to reach for a single seed placed in the well outside of the chamber opening corresponding to their preferred forelimb. Training started once mice were able to successfully retrieve the seed 10 times from the well and lasted 12–13 d. Training consisted of 30 trials or 15 min per day, whichever came first. Per trial, mice were allowed two reach attempts. A reach attempt was counted as a success when the mouse grasped the seed and brought it inside of the chamber to its mouth. Unsuccessful reach attempts included those in which the seed was missed, displaced, or dropped before eating. Training started once mice successfully retrieved 10 seeds. Reaching data were analyzed as successful retrievals per attempt, and for correlations, as the percentage of baseline successful retrievals per attempt. Deficits in reaching performance were probed

Table 1. Primary variables disaggregated by sex[a]

Group (*n*)	Day 3	Week 1	Week 2	Week 3	Week 4	Week 5
Postinfarct reaching success/attempt						
Infarct RT						
Female (3)	0.25 ± 0.01	0.33 ± 0.01	0.34 ± 0.01	0.33 ± 0.01	0.35 ± 0.01	0.40 ± 0.07
Male (3)	0.20 ± 0.02	0.32 ± 0.01	0.43 ± 0.02	0.39 ± 0.01	0.42 ± 0.02	0.42 ± 0.04
Infarct No RT						
Female (4)	0.25 ± 0.02	0.23 ± 0.02	0.31 ± 0.02	0.34 ± 0.02	0.34 ± 0.02	0.40 ± 0.09
Male (4)	0.23 ± 0.01	0.15 ± 0.01	0.20 ± 0.01	0.23 ± 0.03	0.25 ± 0.01	0.28 ± 0.07
Sham RT						
Female (1)	0.41 ± NA	0.43 ± NA	0.46 ± NA	0.44 ± NA	0.51	0.47 ± NA
Male (3)	0.40 ± 0.04	0.36 ± 0.03	0.40 ± 0.06	0.36 ± 0.08	0.40 ± 0.07	0.33 ± 0.04
Sham No RT						
Female (3)	0.34 ± 0.09	0.41 ± 0.01	0.44 ± 0.07	0.38 ± 0.02	0.44 ± 0.2	0.43 ± 0.12
Male (2)	0.34 ± 0.04	0.33 ± 0.03	0.34 ± 0.05	0.34 ± 0.02	0.40 ± 0.08	0.46 ± 0.04
% spine turnover						
Formation	Baseline					
Infarct RT						
Female (3)	2.3 ± 0.1	4.5 ± 0.2	4.0 ± 0.3	5.0 ± 0.3	4.1 ± 0.1	2.7 ± 0.03
Male (3)	2.8 ± 0.03	5.3 ± 0.3	7.3 ± 0.2	5.8 ± 0.1	4.0 ± 0.5	3.3 ± 0.1
Infarct No RT						
Female (4)	2.6 ± 0.03	4.1 ± 0.1	6.8 ± 0.4	4.2 ± 0.3	4.4 ± 0.3	4.9 ± 0.2
Male (5)	2.5 ± 0.1	6.9 ± 0.7	6.3 ± 0.9	4.3 ± 0.3	3.9 ± 0.4	4.4 ± 0.3
Sham RT						
Female (1)	1.2 ± NA	1.4 ± NA	1.4 ± NA	1.4 ± NA	1.8 ± NA	1.8 ± NA
Male (3)	2.2 ± 0.1	2.2 ± 0.1	1.9 ± 0.1	2.4 ± 0.4	1.8 ± 0.3	2.2 ± 0.4
Sham No RT						
Female (2)	2.3 ± 0.5	3.7 ± 0.7	2.2 ± 0.3	2.5 ± 0.4	2.2 ± 0.2	2.0 ± 0.1
Male (1)	2.0 ± NA	1.5 ± NA	3.0 ± NA	2.0 ± NA	1.7 ± NA	1.9 ± NA
Elimination						
Infarct RT						
Female (3)	2.3 ± 0.1	8.4 ± 0.20	6.6 ± 0.4	3.7 ± 0.4	2.5 ± 0.03	3.0 ± 0.07
Male (3)	2.8 ± 0.1	13.0 ± 1.0	6.6 ± 0.5	5.7 ± 0.7	4.2 ± 0.2	3.4 ± 0.07
Infarct No RT						
Female (4)	2.4 ± 0.1	10.7 ± 0.4	6.8 ± 0.3	5.3 ± 0.1	4.5 ± 0.2	5.9 ± 0.2
Male (5)	2.5 ± 0.1	12.1 ± 0.5	7.8 ± 1.7	3.5 ± 0.4	6.0 ± 0.6	4.1 ± 0.8
Sham RT						
Female (1)	1.7 ± NA	1.4 ± NA	1.4 ± NA	1.4 ± NA	2.4 ± NA	1.2 ± NA
Male (3)	2.2 ± 0.1	2.9 ± 0.2	2.0 ± 0.2	2.4 ± 0.4	2.1 ± 0.01	2.5 ± 0.4
Sham No RT						
Female (3)	3.0 ± 0.01	2.7 ± 0.01	2.6 ± 0.01	2.5 ± 0.01	3.2 ± 0.0	2.2 ± 0.0
Male (1)	1.5 ± NA	2.5 ± NA	2.0 ± NA	3.0 ± NA	2.6 ± NA	2.0 ± NA

[a]Data are mean ± SE. *n* values are the same across time points unless otherwise noted.

initially 3 d following photothrombotic infarcts and then once weekly for 5 weeks. Reaching performance was similar across sexes within conditions (Table 1). RT of the preoperatively preferred/paretic forelimb consisted of the same procedures used for preoperative training, and occurred 5 d a week for 4 weeks beginning 5 d after ischemia. At the same time points for no-training control procedures, mice in No RT conditions spent an equal amount of time in the testing chamber as animals receiving RT and were given seeds to eat from the chamber floor, but did not reach for them.

Artery-targeted photothrombosis. For artery-targeted photothrombotic infarcts, mice were anesthetized with isoflurane (4% induction, 1.5%–2% maintenance) in O_2 and affixed to a stereotaxic frame. Arterial oxygen saturation and heart rate from pulse oximetry (MouseOx; Starr Life Sciences) were recorded, and temperature was maintained at 37°C with a feedback temperature control system (FHC). A green diode laser (532 nm, Millenia V, Spectra Physics) was coupled to a digital micro-mirror device (DMD, LDD400–1P, Wavelength Electronics) to provide patterned illumination (20 mW) focused over arterial vessels on the pial surface supplying the forelimb region of M1, with minimal exposure to surrounding parenchyma (Clark et al., 2019). Before baseline imaging, distal branches of the middle cerebral artery over the caudal forelimb area of M1 (Tennant et al., 2015) were identified for photothrombosis from images taken at the time of cranial window implantation. At the time of photothrombosis, between 1 and 2 distal branches of the anterior cerebral artery were also illuminated to control the level of collateral flow at the time of occlusion. Thirty seconds following a retro-orbital injection of Rose Bengal (50 μl, 15 mg/ml i.v., Sigma-Aldrich, catalog #330000), target vessels were irradiated with the patterned laser for 5 min. For Sham procedures, animals were exposed to laser illumination after injections of sterile saline. In all animals, cerebral blood flow (CBF) was monitored in real time for up to 10 min following illumination using traditional laser speckle contrast imaging. As explained below, these data were used to define two photon sample locations relative to the infarct core, as defined by the region of <20% CBF of baseline at 10 min after the infarct. The penumbra area, as defined by the region with CBF between 20% and 70% of baseline at 10 min after the infarct, was similar between groups (mean ± SE, No RT = 6.94 ± 0.49 mm^2, RT = 6.89 ± 0.55 mm^2). Photothrombotic or Sham procedures were performed 1 d following the second baseline imaging session and final preoperative training day.

In vivo *imaging of dendrites.* All imaging was performed under isoflurane anesthesia, which has been shown to increase the mobility of filopodia, but not spines, in cortex *in vivo* (Yang et al., 2011). Animals were anesthetized with 1.5% isoflurane in O_2 and inserted into a custom-made stereotaxic apparatus fitted with a headbar to help minimize breathing artifact. During the first baseline imaging session, 5 or 6 image stacks containing at least 8–10 dendrites with visible spines in each stack were

Table 2. Percentage of new spine maintenance[a]

Group (*n*)	Weeks 1 and 2	Weeks 1–3	Weeks 1–4	Weeks 1–5
Infarct RT				
Female (2)	58.5 ± 4.3	47.2 ± 1.4	47.2 ± 1.4	47.2 ± 1.4
Male (3)	85.6 ± 2.4	58.3 ± 2.8	58.3 ± 2.8	50.0 ± 0
Infarct No RT				
Female (3)	63.6 ± 3.3	41.1 ± 8.0	30.0 ± 5.0	23.2 ± 4.8
Male (4)	66.3 ± 1.7	50.8 ± 1.6	32.5 ± 1.0	28.3 ± 1.5
Sham RT				
Female (1)	100 ± NA	67.7 ± NA	33.3 ± NA	0 ± NA
Male (3)	38.9 ± 5.6	11.1 ± 11.1	0 ± 0 (2)	0 ± 0 (2)
Sham No RT				
Female (2)	58.4 ± 8.4	25.0 ± 8.3	16.7 ± 16.7	1 ± NA
Male (1)	25.0 ± NA	25.0 ± NA	0 ± NA	0 ± NA
		Weeks 2 and 3	Weeks 2–4	Weeks 2–5
Infarct RT				
Female (3)	—	68.3 ± 3.1	53.3 ± 1.1	50.0 ± 0 (2)
Male (3)	—	85.7 ± 2.7	69.0 ± 2.5	69.0 ± 2.5
Infarct No RT				
Female (4)	—	59.4 ± 1.4	43.0 ± 1.7	31.8 ± 2.1
Male (4)	—	62.8 ± 2.1	31.9 ± 1.0	20.5 ± 1.0
Sham RT				
Female (1)	—	100.0 ± NA	50.0 ± NA	0 ± NA
Male (3)	—	44.4 ± 11.1	22.1 ± 11.1	0 ± 0
Sham No RT				
Female (3)	—	53.3 ± 3.3	46.7 ± 3.3	1 ± NA
Male (1)	—	33.3 ± NA	0 ± NA	0 ± NA
			Weeks 3 and 4	Weeks 4 and 5
Infarct RT				
Female (2)	—	—	81.8 ± 0	81.8 ± 0
Male (3)	—	—	73.8 ± 4.8	55.6 ± 1.9
Infarct No RT				
Female (3)	—	—	57.2 ± 4.6	31.4 ± 3.1
Male (5)	—	—	56.2 ± 3.3	40.5 ± 1.6
Sham RT				
Female (0)	—	—	NA ± NA	NA ± NA
Male (2)	—	—	66.6 ± 33.3	16.6 ± 16.6
Sham No RT				
Female (2)	—	—	37.5 ± 12.5	1 ± NA
Male (1)	—	—	66.6 ± NA	50.0 ± NA

[a]Data are mean ± SE. *n* values are the same across time points unless otherwise noted.

selected across distances spanning 300 μm to 1 mm (as measured at the center of each stack) from the middle cerebral arterioles to be targeted for photothrombosis (Fig. 1*B*). This approach extended some of the baseline sample territory into that of the likely infarct core as a strategy to ensure that the remaining samples extended across penumbra. The distance range was selected based on prior findings from the same infarct model in which the infarct core region of severely reduced blood flow (<20%) was found to be surrounded by a penumbra of less severe blood flow reductions that extended ~1 mm from the core (Clark et al., 2019). The infarct core was then estimated using traditional laser speckle contrast imaging as the region with <20% baseline CBF 10 min after the artery-targeted photothrombosis procedure. All samples within 300 μm, and some within 650 μm from the estimated core, were found to be unsuitable for postinfarct spine dynamics analysis due to either the absence of at least eight intact dendrites with distinguishable spines or to gross changes in dendritic fluorescence, presumably stemming from dendritic damage. Thus, the analyses of spine turnover were concentrated between 650 and 1000 μm from the infarct core, as explained in more detail below.

Images were acquired using a Prairie Ultima standard two-photon microscope (Bruker) with a Ti:Sapphire laser tuned to either 860 nm (GFP) or 920 nm (YFP) at low laser power (~30 mW) to minimize phototoxicity. Laser power was adjusted through a Pockels cell to obtain near identical fluorescence at each imaging location and across imaging days. Image stacks were gathered between 50 and 200 μm depths from the pial surface using a water-immersion objective (20×, 1.0 NA, Olympus) and a digital zoom of 4× (Fig. 1 *D*, *E*). Image stacks consisted of 150–200 optical sections spaced 1 μm apart covering an area of 240 μm × 240 μm (512 × 512 pixels, 0.13 μm/pixel). Animals were imaged twice before photothrombosis, with the first imaging session occurring after the seventh day of preoperative behavioral training and the second imaging session following the final training session. Animals were then imaged once a week for up to 5 weeks following ischemic insult (Fig. 1).

Spine dynamics analyses. All analyses of dendritic spine turnover were performed blind to experimental condition. A total of 8–10 intact dendritic segments per image stack, each at least 20 μm in length, were analyzed (~100–200 spines per animal) using ImageJ software (see Fig. 3). Spines were considered to be the same between imaging sessions based on their relative position to adjacent dendrites and spines. Because of lower two-photon resolution in the axial plane, only dendritic spines projecting laterally were included in the analysis. For a spine to be considered new or lost, it had to clearly protrude out of the shaft by at least 4 pixels (0.55 μm), and it could not be part of a dendritic segment that appeared to have significantly rotated or shifted, as judged by any gross changes in the appearance of neighboring spines or branches. Spine turnover was measured by comparing dendritic protrusions in the image being analyzed with those in the previous imaging session. A spine was counted as stable if it appeared in both the previous imaging session and the one being analyzed, as newly formed if it was only present in the image being analyzed, and as eliminated if it was visible in the previous imaging session but not in the one being analyzed. The percentage of spine formation and elimination was calculated as the number of spines gained or lost divided by the total number of stable spines in the analyzed imaging session (Xu et al., 2009). Analyses were performed on raw unprocessed image stacks; but for presentation purposes, images are shown as maximum intensity projections consisting of 5–10 optical sections with median and Gaussian filters applied. Spine turnover was similar across GFP and YFP lines at all times points. For example, in infarct groups, the percentage of spine formation and elimination at baseline was 2.6 ± 0.3 and 2.6 ± 0.4, respectively, in GFP ($n = 4$) and 2.7 ± 0.2 and 2.6 ± 0.1 in YFP ($n = 4$). At week 1 after the infarct, the percentage of spine formation and elimination was 6.0 ± 0.8 and 13.1 ± 1.1 in GFP and 7.9 ± 0.6 and 11.1 ± 1.5 in YFP.

If more than half of an identified dendritic segment contained dendritic blebbing or beading from photothrombosis, it was excluded from the analyses. Changes in fluorescence intensity and dendritic beading between 350 and 650 μm from the infarct core limited the analysis of spine turnover in this region to a subset of the animals (No RT, $n = 4$; RT, $n = 2$). Spine turnover between 651 μm to 1 mm from the infarct core was analyzed in all animals, with the exception of 2 of the 4 No RT subgroup in which closer samples were analyzed, due to restrictions in sample area based on the location of the infarct with respect to window edges. In the 4 animals in which spines were sampled across distances, there was a tendency for spine elimination to be greater in the first 3 weeks after the infarct on closer (350–650 μm) versus further dendrites (mean ± SE: 10.0 ± 1.3% vs 7.7 ± 1.3%), and for spine formation to be greater on closer versus further samples in the last 3 weeks (weeks 3–5: 5.4 ± 1.4% vs 3.8 ± 0.5%); however, spine turnover was not significantly different across distances at any of the imaging time points (p values = 0.06–0.84). The ratio of closer to further spines sampled was matched across No RT (mean ± SE: 0.50 ± 0.18) and RT (0.52 ± 0.35) groups at 1 week after the infarct.

The maintenance of new spines formed during the first through third postinfarct weeks was tracked until the final imaging session (week 5). A criterion for inclusion of individual imaging sessions in analyses of spine maintenance was that at least 3 new spines were counted in the previous imaging session, to counter variability contributed by small samples of new spines without excessive exclusion of low spine turnover conditions. This resulted in some attrition per time point in the Sham group due to low spine turnover in this group ($n = 1$ at weeks 1 and 2, $n = 2$ at week 3) and in infarct groups due to postischemic damage to sample regions at week 1 (No RT, $n = 2$; RT, $n = 1$) or loss of previously analyzed dendrites at week 2 (No RT, $n = 1$) and week 3 (infarct No RT, $n = 1$). To probe for

changes in the overall density of spines on the superficial dendrites imaged *in vivo*, spine density (spines/μm) was measured in two-photon image stacks at baseline and at week 5 on dendrites between 10 and 30 μm in length that were present at both time points. The dendrites sampled were between 650 and 1 mm from the infarct core.

Tissue processing and histological analyses. Eight weeks after the infarcts or Sham procedures, all animals were overdosed with sodium pentobarbital and transcardially perfused with 0.1 M PBS and 4% PFA. Following fixative perfusion, brains were extracted and stored in 4% PFA for <48 h before being sliced into 40-μm-thick coronal sections using a VT1000S vibratome (Leica Microsystems). All histological measures were made on tissue that was coded to blind for experimental condition.

Every sixth section was mounted onto gelatin-coated slides and Nissl-stained with toluidine blue. Contralesional and remaining ipsilesional cortical areas were measured in eight coronal sections per animal between ~1.34 mm anterior and 0.58 mm posterior to bregma spaced 240 μm apart. Area measures were made with Neurolucida software at a final magnification of 17×. Cortical volume was estimated as the product of summed section areas and the distance between sections. Lesion volume was then calculated as the difference between volumes of the contralesional and ipsilesional cortices (Tennant et al., 2015).

One set of coronal sections was mounted on glass slides for visualization of spine density on YFP$^+$ and GFP$^+$ pyramidal neurons using confocal microscopy. Image stacks were acquired using the confocal mode on the two-photon microscope. The dichroic mirror was replaced with a lens tuned to 488 nm (FITC), and image stacks containing apical dendritic branches within layer II/III (between 200 and 400 μm from the surface) of motor cortex were gathered using a water-immersion objective (20×, 1.0 NA, Olympus). Spine density analyses were performed using ImageJ software. A total of 8–10 apical dendrites measuring at least 50 μm in length were sampled between 300 μm and 1 mm from the edge of the core in the ipsilesional hemisphere. In Sham animals, samples homotopic to the lesion site within the trained (ipsilesional) M1 were gathered. Data from 4 animals (infarct RT, $n = 1$; infarct No RT, $n = 2$; Sham No RT, $n = 1$) had to be omitted due to an inability to localize a sufficient sample of dendrites of this length. For all dendritic analyses, spines along the length of measured dendrite were manually counted, and density was calculated as total spines per length of dendrite (spines/μm).

Statistical analyses. All statistical analyses were performed using the SPSS software package (IBM, RRID:SCR_002865). We expected preliminary analyses to justify the combination of Sham subgroups (RT vs No RT) for statistical comparisons with infarct groups because the Sham RT condition consisted of practice on a previously established task, which does not influence spine turnover on the dendrites examined (in contrast to training on a novel task) (Xu et al., 2009; Clark et al., 2018). As expected, there were no significant differences between Sham subgroups in spine turnover (main effect: $F_{(1,6)} = 2.50$, $p = 0.29$; interaction: $F_{(3,18)} = 1.20$, $p = 0.33$) or spine elimination (main effect: $F_{(1,6)} = 3.42$, $p = 0.33$; interaction: $F_{(3,18)} = 0.51$, $p = 0.67$), and they were combined for remaining analyses. Males and females were also combined for the statistical analyses, but descriptive results for the primary variables in subgroups separated by sex can be found in Tables 1 and 2.

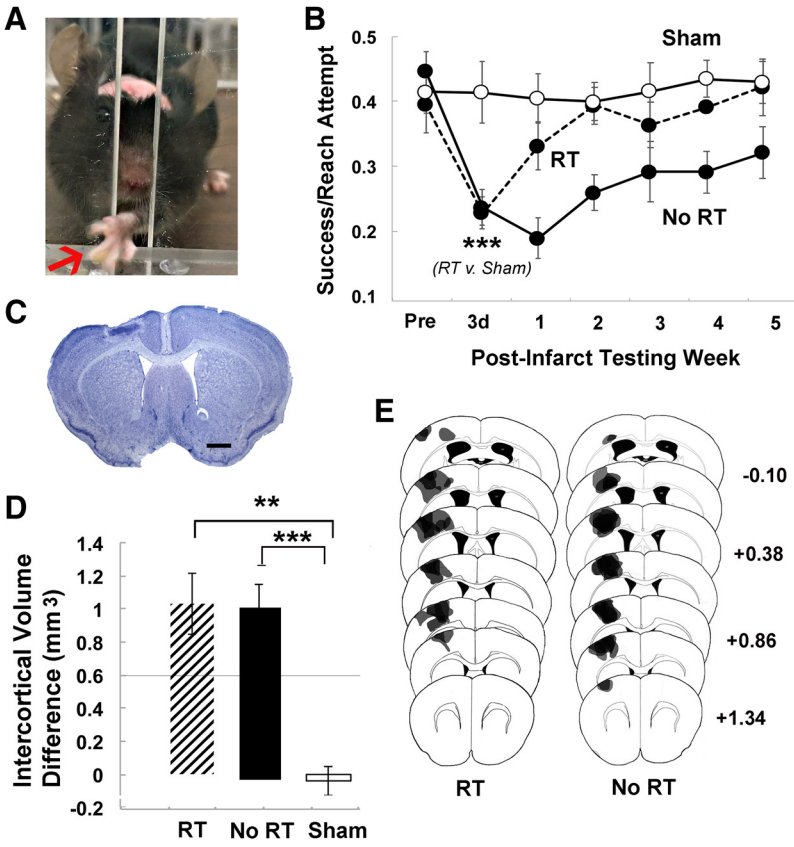

Figure 2. RT improved postinfarct skilled reaching performance. ***A***, Example of a mouse performing the single-seed retrieval task. The arrow points to the seed, which is grasped between digits. ***B***, Reaching performance, measured as successful retrievals per reach attempt. Postinfarct performance significantly declined in both infarct groups. In the No RT group, performance decrements relative to Sham did not vary significantly by time over the 5 weeks after the infarct. In contrast, the RT group performed significantly worse than Sham only at postinfarct day 3 and not thereafter. ***C***, Representative lesion in a Nissl-stained coronal section. Scale bar, 500 μm. ***D***, Cortical lesion volume, measured as the difference in cortical volume between ipsilesional and contralesional hemispheres, was similar between the No RT and RT groups. The intercortical volume difference in both infarct groups was significantly greater than Sham. ***E***, Representative lesion reconstructions of the infarct group overlaid on coronal section templates. Numbers to the right indicate anterior to posterior coordinates in millimeters relative to bregma. Data are mean ± SE. $^{**}p < 0.01$ versus Sham. $^{***}p < 0.0001$ versus Sham.

The effect of postinfarct RT on spine dynamics was examined using a repeated-measures ANOVA with infarct group (RT vs No RT) as a between-subjects variable and time as a within-subjects variable. Each infarct group was additionally compared with Sham in separate ANOVAs. The Shapiro–Wilks test was used to check for normality. When warranted by significant group × time interactions, *post hoc* group comparisons per time point were performed using Holm–Bonferroni-corrected two-tailed *t* tests. Separate repeated-measures ANOVAs comparing the groups outlined above were used to examine infarct and RT effects on the maintenance of spines formed during weeks 1, 2, and 3 after the infarct. The last imaging time point (week 5) was omitted from the spine dynamics ANOVA because of animal attrition at this time point, but between-group comparisons at this time point were analyzed with *t* tests, and this time point was counted as a comparison in the Bonferroni–Holm's correction when *post hoc* tests per time point were warranted by ANOVA results.

Repeated-measures ANOVAs were used to probe for differences in postinfarct reaching performance over time using the same group comparisons as above; and when warranted by ANOVAs, *post hoc* Bonferroni-corrected *t* tests were used to probe differences at individual time points between groups. Differences in spine density at 8 weeks after operation were assessed using independent-samples two-tailed *t* tests.

In secondary analyses motivated by the primary ANOVA results, Pearson correlations were used to probe for relationships between postinfarct

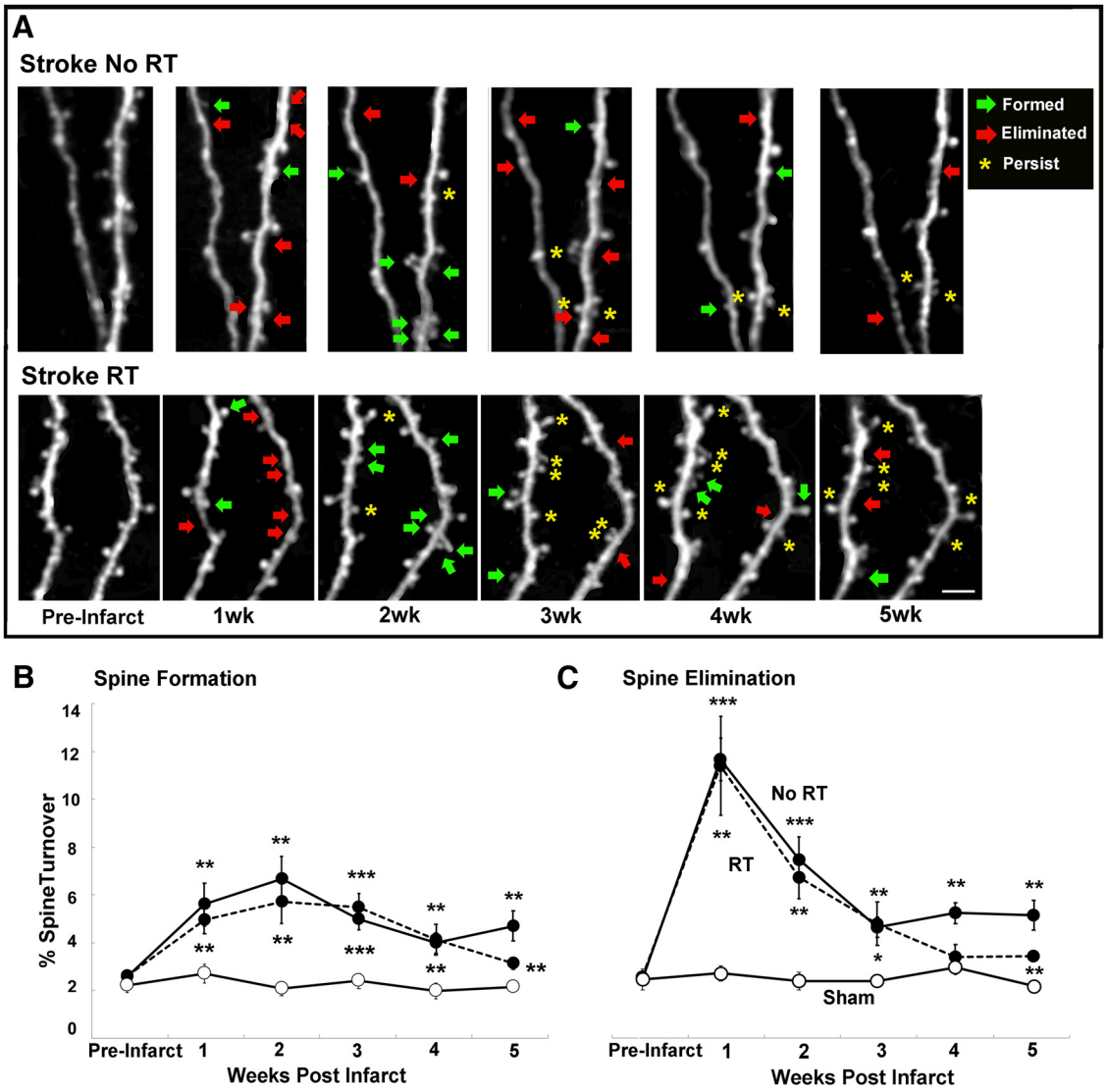

Figure 3. Patterns of spine turnover in peri-infarct cortex. ***A***, Examples of spine turnover in peri-infarct cortex over 5 weeks. Scale bar, 10 μm. ***B***, Spine formation was increased in both infarct groups relative to Sham across all postinfarct weeks. ***C***, Spine elimination was increased in both infarct groups relative to Sham at each time point, with the exception of week 4 in RT. Infarct groups did not differ significantly from one another, with the exception of week 5, when spine formation and elimination were significantly lower in the RT versus the No RT group (for details, see text). Data are mean ± SE. *$p < 0.02$ versus Sham. **$p < 0.001$ versus Sham. ***$p < 0.0001$ versus Sham.

reaching performance and new spine survival in each training condition. Reaching performance improvements relative to baseline at weeks 2, 3, and 4 were related to the persistence of new spines that appeared in preceding weeks. Week 5 was not included due to animal attrition at that time point. Week 2 was chosen as the first time point corresponding to near baseline performance in the RT group. The correlation between percentage baseline reaching performance at week 4 and layer II/II spine density was also assessed.

Results

RT improved deficits in skilled reaching

Focal ischemic infarcts to mouse motor cortex impair skilled reaching behavior in the contralateral forelimb (Balkaya et al., 2013; Clarkson et al., 2013; Tennant et al., 2015). In the present study we found that artery-targeted photothrombotic infarcts of M1 in mice significantly impaired performance of a previously acquired skilled reaching task (Fig. 2). In mice that received RT of the impaired limb on the same reaching task performance recovered to near baseline levels within 2 weeks while postinfarct performance in the No RT group remained lower than baseline through the 5 weeks of testing (Fig. 2*B*). ANOVA for postinfarct performance between RT and No RT groups revealed a significant main effect of group ($F_{(1,11)} = 6.71$, $p = 0.03$) but not a group × time interaction ($F_{(4,44)} = 2.26$, $p = 0.07$), reflecting superior performance in the RT group throughout the RT period.

Infarct groups also varied in postinfarct performance patterns relative to Sham. In repeated-measures ANOVA, postinfarct performance in the No RT group was significantly impaired overall compared with Sham (main effect of group: $F_{(1,14)} = 7.56$, $p = 0.006$), an effect that did not vary significantly with time (group × time interaction: $F_{(4,56)} = 0.47$, $p = 0.87$). In contrast, between RT and Sham groups, there was a significant group × time interaction ($F_{(4,56)} = 3.30$, $p = 0.02$), but not a main effect of group ($F_{(1,14)} = 4.26$, $p = 0.06$), reflecting the transience of the impaired reaching performance in the RT group. *Post hoc* Bonferroni *t* tests confirmed that, compared with Sham, the RT group performed significantly worse on postinfarct day 3 ($t_{(13)} = 2.16$, $p = 0.004$) but not at any other time point (Fig. 2*B*). Lesion volumes and extent (Fig. 2*C–E*) were similar between infarct

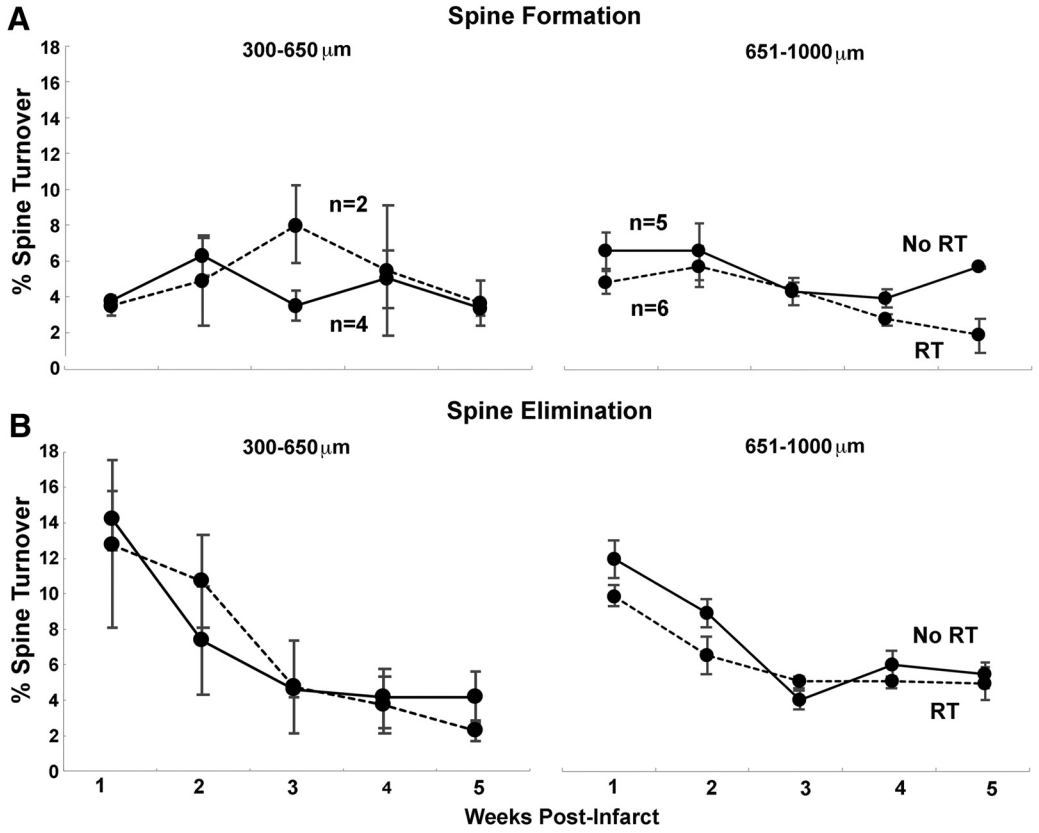

Figure 4. The general pattern of spine turnover was similar across distances. The pattern of spine formation (***A***) and elimination (***B***) in infarct groups at closer (300–650 μm) and further (651–1000 μm) distances from the infarct core over time. There were no significant differences across distances. Data are mean ± SE.

groups and did not substantially vary across males (mean ± SE*:* 1.03 ± 0.36 and 1.01 ± 0.17 mm^3 in RT and No RT, respectively) and females (0.86 ± 0.07 and 0.80 ± 0.16). These results support that RT improved postinfarct recovery of reaching performance.

Artery-targeted photothrombosis similarly increased spine turnover in peri-infarct cortex with and without RT

Sustained increases in spine turnover have been observed in peri-infarct cortex in the absence of any postinfarct behavioral intervention (Brown et al., 2007, 2010). Endpoint histological analyses have revealed that rehabilitative training after focal ischemic lesions to motor cortex increases spine and synapse density, synapse maturation, and dendritic complexity in the remaining motor cortex (Wang et al., 2016; Kim et al., 2018), but its impact on spine dynamics was unknown. That increased spine turnover is likely to be ongoing during RT in a region where it promotes synaptic structural changes raised the possibility that synaptic structural responses to RT reflect, in part, interactions with spine turnover responses.

In the present study, we found robust elevations in spine turnover in peri-infarct motor cortex that were generally similar in the RT and No RT groups relative to Sham. Spine formation (Fig. 3*B*) and elimination (Fig. 3*C*) were elevated in both infarct groups during the 5 weeks following ischemia relative to Sham animals. Repeated-measures ANOVAs over this time period revealed significant main effects of each infarct group relative to Sham in the percentage of spines formed (No RT: $F_{(1,14)} = 141.70$, $p < 0.0001$; RT: $F_{(1,12)} = 41.10$, $p < 0.0001$) and the percentage of spines eliminated (No RT: $F_{(1,14)} = 121.30$, $p < 0.0001$; RT: $F_{(1,12)} = 37.24$, $p < 0.0001$) as well as significant group × time interactions for each measure (spine formation: No RT: $F_{(3,42)} = 15.96$, $p < 0.0001$; RT: $F_{(3,36)} = 17.27$, $p < 0.0001$; spine elimination: No RT: $F_{(3,42)} = 17.35$, $p < 0.0001$; RT: $F_{(3,36)} = 24.45$, $p < 0.0001$), reflecting partial resolution of postischemic elevations in spine turnover over time. The RT group tended to show greater return to baseline levels of spine turnover near the end of the observation period than did the No RT group. However, Bonferroni-corrected *t* tests indicated that spine formation (Fig. 3*B*) was significantly greater than Sham in both infarct groups at each postinfarct time point, as was spine elimination with the exception of week 4 in the RT group (Fig. 3*C*). Given that repeated anesthesia did not alter spine dynamics in either Sham group, it is unlikely that the effects of photothrombosis and rehabilitative training on spine dynamics were greatly influenced by the use of isoflurane anesthesia.

In comparing spine turnover between infarct groups, ANOVA revealed that the pattern of spine formation (group × time: $F_{(3,36)} = 0.42$, $p = 0.73$; main effect: $F_{(1,12)} = 0.25$, $p = 0.62$) and spine elimination (group × time: $F_{(3,36)} = 0.50$, $p = 0.67$; main effect $F_{(1,12)} = 0.70$, $p = 0.41$) were similar over the first 4 weeks after the infarct between RT and No RT groups. Only at the week 5 time point was spine turnover significantly different, higher in the No RT compared with RT group in independent-samples *t* tests (Fig. 3; formation: $t_{(9)} = 2.26$, $p = 0.024$; elimination: $t_{(9)} = 2.26$, $p > 0.02$). The patterns of spine turnover on dendrites that were more proximal (350–650 μm) and distal (650–1000 μm) to the infarct core were also generally similar between groups (Fig. 4). Together, these results indicate that

RT had little impact on postischemic patterns of spine turnover in peri-infarct motor cortex, other than to subtly speed its resolution.

RT promoted new spine stabilization

We next examined the persistence of new spines that were formed during the initial weeks after the infarct. We found that RT was associated with greater maintenance of spines formed during the first 3 weeks after the infarct relative to both No RT and Sham animals (Fig. 5). As shown in Figure 5*A*, the maintenance of spines formed in postinfarct week 1 through the subsequent 3 weeks was not significantly different between RT and No RT groups (ANOVA main effect of group: $F_{(2,20)} = 2.37$, $p = 0.12$; group × time interaction: $F_{(1,10)} = 1.93$, $p = 0.19$). However, by week 5, there was a significantly greater percentage of the spines remaining in RT compared with No RT (independent-samples *t* test: $t_{(2,7)} = 2.36$, $p = 0.02$). The No RT group was not significantly different from Sham in the maintenance of new spines formed during week 1 (ANOVA for weeks 2–4, group: $F_{(1,11)} = 2.76$, $p = 0.12$; group × time: $F_{(2,22)} = 1.14$, $p = 0.33$; week 5: $t_{(2,9)} = 2.26$, $p = 0.12$). In contrast, between the RT and Sham groups, there was both a significant group × time interaction ($F_{(2,18)} = 3.81$, $p = 0.04$) and significant main effect of group ($F_{(1,9)} = 7.89$, $p = 0.02$). Bonferroni-corrected *t* tests revealed that spine maintenance was greater in the RT group compared with Sham at week 4 ($t_{(2,6)} = 2.44$, $p = 0.003$) and week 5 ($t_{(2,10)} = 2.22$, $p = 0.001$), indicating that RT promoted greater long-term persistence of spines that were formed during the first week after the infarct (Fig. 5*A*).

RT also increased the persistence of new spines formed during postinfarct weeks 2 and 3 (Fig. 5*B*,*C*). In No RT and Sham groups, the majority of new spines formed in weeks 2 and 3 had disappeared by week 4, whereas the majority remained in the RT group through week 5. The maintenance of spines formed in week 2 (Fig. 5*B*) was significantly increased in the RT group relative to the No RT group ($F_{(1,12)} = 8.0$, $p = 0.01$), an effect that did not vary significantly across weeks 3 and 4 (group × time interaction, $F_{(1,12)} = 0.74$, $p < 0.4$) and which continued to be significant at week 5 ($t_{(2,11)} = 2.20$, $p = 0.004$). The maintenance of spines formed during week 2 was also increased in the RT group relative to Sham (ANOVA for weeks 3 and 4, group: $F_{(1,11)} = 6.8$, $p = 0.02$, group × time: $F_{(1,11)} = 2.31$, $p = 0.15$; *t* test for week 5: $t_{(2,8)} = 2.30$, $p = 0.002$). In contrast, the No RT group lost spines that were formed in week 2 at a rate similar to, and not significantly different from, the Sham group (ANOVA for weeks 3 and 4, group: $F_{(1,13)} = 0.001$, $p = 0.97$; group × time: $F_{(1,13)} = 0.22$, $p = 0.64$; *t* test for week 5: $t_{(2,8)} = 2.30$, $p = 0.002$). For spines formed during week 3, independent-samples *t* tests revealed that spine maintenance at week 5 was significantly greater in the RT group compared with both No RT ($t_{(2,10)} = 2.20$, $p = 0.01$) and Sham ($t_{(2,7)} = 2.36$, $p = 0.02$), but not between the No RT group and Sham ($t_{(2,10)} = 2.23$, $p = 0.26$; Fig. 3*C*). Together, these results indicate that RT promoted the maintenance of spines that were formed in peri-infarct cortex during the first 3 weeks after the infarct.

Given that RT was associated with a greater maintenance of new spines formed after the infarct, we additionally assessed whether this was reflected in an increase in the net quantities of spines at the 5 week time point by examining spine density (spines/μm) on the subset of apical dendrites imaged *in vivo* that were present at both baseline and week 5 (Table 3). In both groups, spine density at week 5 was subtly, but significantly, decreased from spine density at baseline (No RT paired, $t_{(1,6)} = 2.36$, $p = 0.001$; and RT, $t_{(1,4)} = 2.77$, $p = 0.01$). However, the within-animal reduction in spine density between week 5 and baseline was significantly lower in the RT group compared with No RT group ($t_{(2,11)} = 2.20$; Table 3). Thus, RT was associated with a greater normalization in spine density at the 5 week time point.

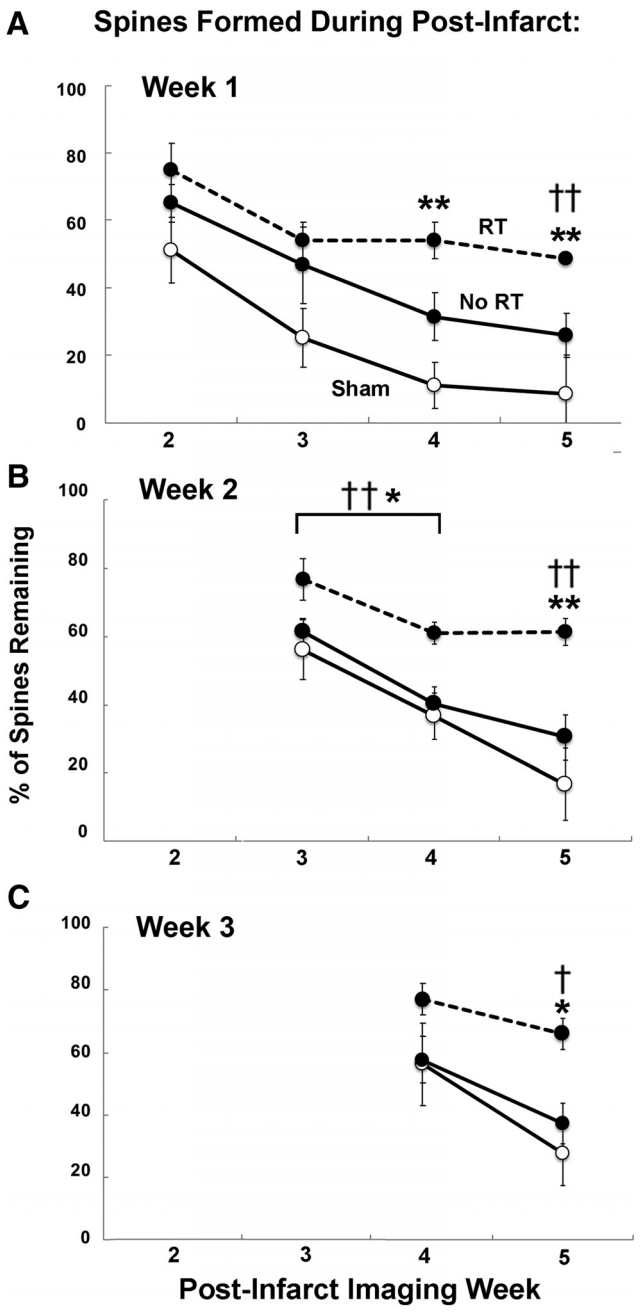

Figure 5. Long-term maintenance of spines formed during postinfarct weeks 1–3 was greater with RT. ***A***, Percentage of new spines formed during postinfarct week 1 that remained in weeks 2–5. A greater percentage of spines persisted to the final time point in the RT group compared with No RT and Sham. ***B***, The percentage of spines formed during week 2 that persisted in weeks 3–5 was greater overall in RT compared with No RT and Sham (for details, see text). ***C***, The percentage of spines formed during week 3 that remained at week 5 was greater in RT compared with No RT and Sham. Data are mean ± SE. †$p < 0.05$, RT versus No RT. ††$p <$ 0.01, RT versus No RT; *$p < 0.05$, RT versus Sham. **$p < 0.01$, RT versus Sham.

Table 3. Layer I dendritic spine density per micrometer[a]

Group (*n*)	Baseline	Week 1	Week 2	Week 3	Week 4	Week 5	Baseline − week 5
No RT (7)	0.34 ± 0.004	0.29 ± 0.01	0.29 ± 0.01	0.28 ± 0.01	0.29 ± 0.01	0.28 ± 0.01*	0.05 ± 0.009**
RT (5)	0.32 ± 0.01	0.29 ± 0.01	0.29 ± 0.01	0.30 ± 0.01	0.31 ± 0.01	0.31 ± 0.01*	0.02 ± 0.002

[a]Data are mean ± SE.

*$p < 0.01$ versus baseline; **$p = 0.01$ versus RT.

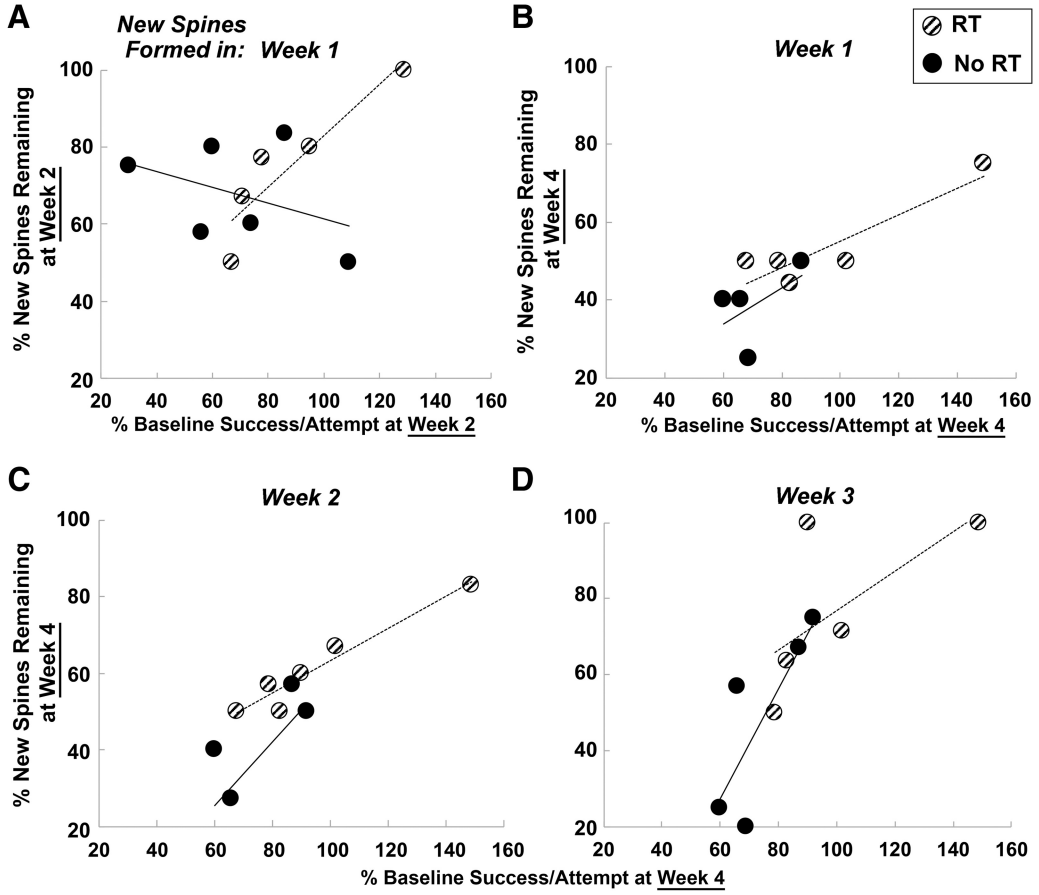

Figure 6. Stabilization of spines formed during weeks 1 and 2 after the infarct predicted RT-promoted reaching performance improvements. Relationships between reaching performance at weeks 2 and 4 and the persistence of spines formed in the preceding weeks. Performance was analyzed as the percentage preoperative baseline successful retrievals per reach attempt. ***A***, The percentage of new spines formed during week 1 that persisted to week 2 was significantly correlated with reaching performance at week 2 in the RT, but not in the No RT, group. Similarly, reaching performance in week 4 in the RT, but not the No RT, group was significantly correlated with new spines remaining at week 4 that formed in (***B***) week 1 and (***C***) week 2. ***D***, Relationships between behavior at week 4 and new spines persisting to that point that had formed in week 3 failed to reach significance in both groups (statistical details in text).

The maintenance of new spines in peri-infarct cortex predicted reaching performance

We next examined whether the preferential stabilization of spines formed after the infarct was related to postinfarct reaching performance, as measured by the percentage of baseline performance (Fig. 6). We first examined the relationship between new spine maintenance at week 2 with behavioral performance at week 2 because the RT group returned to near baseline levels of reaching performance at this time point. We found that the percentage of spines formed during week 1 after the infarct remaining at week 2 was significantly correlated with behavior at the same time point in the RT group ($r = 0.91$, $t_{(4)} = 4.61$, $p = 0.009$) but not in the No RT group ($r = -0.40$, $t_{(5)} = 0.99$, $p = 0.37$; Fig. 6*A*). The percentage of spines formed during each of the first 2 weeks after the infarct that remained at week 3 was also positively correlated with behavioral performance at week 3 in the RT group, significantly so for spines formed in week 2 (week 1 new spines: $r = 0.75$, $t_{(4)} = 2.3$, $p = 0.08$; week 2 new spines: $r = 0.89$, $t_{(5)} = 4.82$, $p = 0.006$) but not in the No RT group (week 1 new spines: $r = 0.02$, $t_{(4)} = 0.04$, $p = 0.96$; week 2 new spines: $r = -0.04$, $t_{(4)} = 0.09$, $p = 0.93$). Finally, we found that the percentage of spines formed during each of the first 2 weeks after the infarct that persisted to week 4 was significantly correlated with reaching performance at week 4 in the RT group (Fig. 6*B*,*C*; new spines formed in week 1: $r = 0.90$, $t_{(4)} = 4.24$, $p = 0.01$; new spine formed in week 2: $r = 0.98$, $t_{(4)} = 7.21$, $p = 0.001$), but not in the No RT group (new spines formed in week 1: $r = 0.52$, $t_{(3)} = 1.05$, $p = 0.36$; new spine formed in week 2: $r = 0.66$, $t_{(4)} = 1.79$, $p = 0.17$). The correlation between the percentage of spines formed during week 3 that remained until week 4 of with behavior at week 4 (Fig. 6*D*) failed to reach significance in both the RT ($r = 0.66$, $t_{(4)} = 1.76$, $p = 0.15$) and No RT ($r = 0.80$, $t_{(4)} = 2.32$, $p = 0.09$) group. Thus, in animals receiving RT, there were strong relationships between both early and subsequently maintained improvements in skilled reaching performance and the persistence of spines formed in early postinfarct weeks. The modest

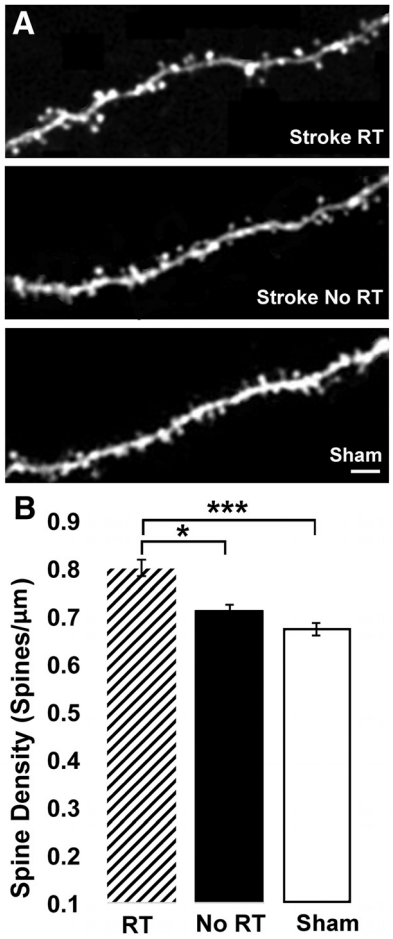

Figure 7. RT increased spine density on apical dendrites of layer V pyramidal neurons in layer II/III of peri-infarct MC. ***A***, Confocal image of an apical dendrite sampled in layer II/III from the RT (top), No RT (middle), and Sham (bottom). Scale bar, 10 μm. ***B***, Spine density, measured as spines/μm, was increased in the RT group at 8 weeks after the infarct relative to both No RT (*$p < 0.05$) and Sham (***$p < 0.0001$). Spine density was not significantly increased in the No RT group compared with Sham ($p = 0.07$).

performance improvements of the No RT group over the same time period were not strongly related to new spine persistence. These data indicate that RT-driven improvements in skilled reaching performance were predicted by the maintenance of new spines.

RT increased spine density on apical dendrites in layer II/III of peri-infarct cortex

We previously found that patterns of motor skill learning-related spine structural plasticity vary across superficial versus deeper apical dendrites of layer V pyramidal neurons (Clark et al., 2018). Training intact mice on a skilled reaching task was associated with spine turnover and selective new spine maintenance, without net increases in spine density, on superficial apical tufts in layer I, whereas spine density increased on apical dendrites in layer II/III, on the same population of layer V pyramidal neurons in the trained M1 (Clark et al., 2018). This motivated our examination in the present study of the impact of RT on spine density in peri-infarct MC along layer II/III apical dendrites (Fig. 7) of the same layer V pyramidal neuron population of which the superficial apical tufts of layer I were imaged *in vivo*. At 8 weeks after the infarct, layer II/III apical dendritic spine density in the RT group was increased compared with the No RT group ($t_{(10)} = 2.23$, $p = 0.002$) and Sham ($t_{(11)} = 2.20$, $p < 0.0001$; Fig. 7*B*). In contrast, spine density was not significantly increased in the No RT group relative to Sham ($t_{(13)} = 2.16$, $p = 0.075$). Spine density on layer II/III dendrites was positively, but not significantly, correlated with behavioral performance (percentage of baseline) at week 4 in the RT group (RT: $r = 0.70$, $t_{(4)} = 1.99$, $p = 0.11$; No RT: $r = 0.35$, $t_{(4)} = 0.75$, $p = 0.49$). Spine density per mm^3 was similar across males and females of the RT (0.82 ± 0.01 and 0.76 ± 0.01, respectively) and No RT (0.72 ± 0.02 and 0.71 ± 0.01) groups. These results suggest that RT promotes synapse addition on layer II/III apical dendrites of layer V pyramidal neurons in peri-infarct cortex, in addition to is promotion of the maintenance of newly formed synapses on more superficial apical dendrites of the same neuronal population.

Discussion

The efficacy of poststroke motor RT has been linked with structural and functional reorganization of the damaged hemisphere (Murphy and Corbett, 2009; Jones and Adkins, 2015). RT-induced improvements in paretic forelimb function after subtotal infarcts of primary motor cortex (M1) are linked with reorganization of residual motor cortical maps in rodents and monkeys (e.g., Nudo et al., 1996; Tennant et al., 2015) and increased density and maturation of synapses in peri-infarct cortex of rats (Kim et al., 2018). However, these changes were observed after RT had promoted considerable behavioral improvements, and the processes by which they occur has not been well explored. Cortical ischemia instigates a period of dramatic synapse turnover in peri-infarct cortex, as revealed by repeated *in vivo* imaging of dendritic spines (Brown et al., 2007, 2010; Mostany and Portera-Cailliau, 2011). Here we investigated the possibility that RT affects synaptic connectivity in peri-infarct cortex via interaction with ischemia-instigated synapse remodeling responses. We followed spine turnover and motor performance in mice undergoing RT or No RT after artery-targeted photothrombotic infarcts of M1. RT improved reaching performance with the paretic forelimb, which recovered to near baseline levels by 2 weeks after the infarct, compared with No RT. We also found robust elevations in spine turnover in peri-infarct cortex lasting up to 5 weeks after the infarct, the pattern of which was generally similar with and without RT with the exception of greater normalization of spine dynamics by week 5 with RT. However, RT significantly increased the stabilization of new spines formed during the first 3 weeks after the infarcts relative to both Sham and No RT. This supports that RT can affect synaptic connectivity in residual M1 by interacting with ischemia-instigated synaptic structural remodeling responses. Furthermore, RT-driven improvement in reaching performance was positively correlated with the maintenance of new spines. These correlative results, together with the experimental results, point to the promotion of greater new spine stabilization by RT as a potential mechanism underlying RT-driven improvements in paretic forelimb function.

That RT interacts with postischemic spine turnover raises the possibility that this contributes to time sensitivities in RT efficacy (Allred et al., 2014). Studies in rodent models support that earlier versus later poststroke onsets of RT can be more effective in improving function (e.g., Biernaskie et al., 2004; Zeiler and Krakauer, 2013). For example, Biernaskie et al. (2004) found that RT initiated 5 d postinfarct in rats promoted greater improvements in reaching performance compared with RT beginning at 14 or 30 d. Although the clinical evidence for time dependencies in upper limb RT efficacy is presently scarce, there is much recent research interest in the topic (Bernhardt et al., 2017; Coleman et

al., 2017), and one study found greater functional improvement in human stroke survivors when the intensive RT approach, constraint induced movement therapy, was initiated in earlier versus later poststroke months (Lang et al., 2013). In the present study, the 5 week period of elevated spine turnover observed could reflect a window of opportunity that facilitates the capacity of RT to shape cortical connectivity, via promotion of new spine stabilization, to subserve practice-dependent improvements in motor function. If so, RT initiated early enough to overlap with the peak period of turnover (first 3 weeks), and to maximize the duration of that overlap, might maximize RT influences on synaptic connectivity in peri-infarct cortex. These possibilities remain to be tested. There is also a need to much more thoroughly investigate the nature of the postinfarct behavioral improvements that are related to new spine stabilization, including potential relationships to spontaneous recovery that the reaching performance measure of the present study could have missed and/or that may have been still to emerge, as well as how relationships may vary across varied individual and stroke characteristics.

Among previous studies to monitor synaptic structural responses to focal ischemia over time, Brown et al. (2007) found robust increases in dendritic spine turnover that persisted up to 6 weeks after traditional photothrombotic infarcts. Increased spine turnover was mostly restricted to within 300 μm of the infarct, approximately the size of the ischemic penumbra in this model (Clark et al., 2019). Mostany and Portera-Cailliau (2011) reported more widespread increases in spine turnover after middle cerebral artery occlusion, which produces a larger penumbra. The artery-targeted photothrombotic approach of the present study enlarges the ischemic penumbra relative to traditional photothrombosis (Clark et al., 2019) and resulted in similarly profound increases in spine turnover on dendrites closer (300–650 μm) and more distant (650–1000 μm) from the infarct core. These results across stroke models are consistent with the spatial area of ischemia-instigated spine turnover in cortex varying with the size of the penumbra.

In comparing the spatial extent of spine turnover across the artery targeted and traditional photothrombosis models, it is important to consider that the former does not generate as sharply delineated lesion borders. This is reflected in the difference between the present study and Brown et al. (2010) in how the infarct zone was defined. Brown et al. (2010) defined it by the absence of fluorescently labeled dendrites, whereas we defined it as the cortical region with <20% baseline CBF 10 min after ischemia induction. This was intended to the define the core, rather than outer limits, of damage, as there is more superficial damage beyond this (Clark et al., 2019), consistent with the lack of sufficiently intact dendrites to sample within 300 μm of the defined infarct core in the present study. Although few of these proximal samples lacked fluorescently labeled dendrites entirely, if we nevertheless considered them part of the infarct zone, the spatial extent of the observed spine turnover responses continues to exceed that of traditional photothrombosis.

Synaptic structural responses to RT are not specific to superficial dendrites imaged *in vivo*. Kim et al. (2018) found that RT increased axodendritic synaptic densities in layer V of peri-infarct M1, including increases in a mature synapse subtype (perforated synapses), which predicted paretic forelimb improvements. In the present study, we found that RT increased spine density on apical dendrites of layer V pyramidal neurons in layer II/III of peri-infarct M1 at 8 weeks postinfarct compared with No RT. Together, these findings indicate synaptic structural responses to RT across at least much of the depth of cortex. That spine density in layer II/III was only modestly correlated with reaching performance at week 4 is also consistent with findings by Kim et al. (2018) that mature, but not overall, synapse quantities in layer V strongly predicted paretic forelimb function. RT effects on new spine stabilization on superficial dendrites, which did predict functional improvements, are likely to also reflect its promotion of synapse maturation. New spines that are stabilized during motor skill learning increase in size (Fu et al., 2012), which is linked with increased synapse strength (Yasumatsu et al., 2008; Hofer et al., 2009; Roberts et al., 2010).

In contrast to its effects in layer II/III at 8 weeks postinfarct, RT did not increase spine densities on the superficial dendrites of the same neuronal population that were imaged *in vivo*, as assessed at 5 weeks postinfarct. While we cannot rule out the contribution of time to these differences in the present study, they bear strong resemblance to laminar dependencies in motor skill learning effects in intact mice, which is associated with increased spine density in layer II/III and increased new spine stabilization, but not density, in layer I, both as assessed at 2 weeks after training (Clark et al., 2018). Together, the findings suggest variation in the structural responses to motor skill training across nearby dendritic subpopulations of the same neurons and are generally consistent with the possibility that both could mediate motor functional improvements.

There is a need to better understand mechanisms of RT efficacy to inform strategies for its improvement. Ischemic stroke instigates neuroregenerative reactions (Cramer and Chopp, 2000; Carmichael, 2006; Brown et al., 2007) that are activity-dependent (Yu and Zuo, 2011; Allred et al., 2014; Tennant et al., 2017), and potentially shaped by behavioral interventions to improve function, but what exactly to target is quite unresolved. Here, we explored whether postischemic synapse remodeling responses might be such a target. Using two-photon imaging to track spine turnover in peri-infarct cortex of mice with and without RT, we found that, while the general spine turnover pattern was not strongly affected, RT greatly increased the persistence of newly formed spines, which correlated with motor performance improvement across training conditions. The stabilization of new spines in peri-infarct cortex potentially represents a structural substrate for RT-driven functional improvements in the paretic forelimb. That RT also increased spine density on the deeper apical dendrites of the same neuronal population, together with prior findings of RT effects in layer V (Kim et al., 2018), is consistent with RT influencing synaptic structure across the depth of cortex. To our knowledge, these results provide the first evidence that RT interacts with postischemic synapse turnover to shape synaptic connectivity in the living brain, and raise the possibility that this interaction could be a therapeutic target for facilitating RT efficacy.

References

Allred RP, Kim SY, Jones TA (2014) Use it and/or lose it: experience effects on brain remodeling across time after stroke. Front Hum Neurosci 8:379.

Balkaya M, Kröber JM, Rex A, Endres M (2013) Assessing post-stroke behavior in mouse models of focal ischemia. J Cereb Blood Flow Metab 33:330–338.

Bernhardt J, Godecke E, Johnson L, Langhorne P (2017) Early rehabilitation after stroke. Curr Opin Neurol 30:48–54.

Biernaskie J, Chernenko G, Corbett D (2004) Efficacy of rehabilitative experience declines with time after focal ischemic brain injury. J Neurosci. 24:1245–1254.

Brown CE, Li P, Boyd JD, Delaney KR, Murphy TH (2007) Extensive turnover of dendritic spines and vascular remodeling in cortical tissues recovering from stroke. J Neurosci 27:4101–4109.

Brown CE, Boyd JD, Murphy TH (2010) Longitudinal in vivo imaging re-

veals balanced and branch-specific remodeling of mature cortical pyramidal dendritic arbors after stroke. J Cereb Blood Flow Metab 30:783–791.

Carmichael ST (2006) Cellular and molecular mechanisms of neural repair after stroke: making waves. Ann Neurol 59:735–742.

Castro-Alamancos MA, Borrel J (1995) Functional recovery of forelimb response capacity after forelimb primary motor cortex damage in the rat is due to the reorganization of adjacent areas of cortex. Neuroscience 68:793–805.

Clark TA, Fu M, Dunn AK, Zuo Y, Jones TA (2018) Preferential stabilization of newly formed dendritic spines in motor cortex during manual skill learning predicts performance gains, but not memory endurance. Neurobiol Learn Mem 152:50–60.

Clark TA, Sullender C, Kazmi SM, Speetles BL, Williamson MR, Palmberg DM, Dunn AK, Jones TA (2019) Artery targeted photothrombosis widens the vascular penumbra, instigates peri-infarct neovascularization and models forelimb impairments. Sci Rep 9:2323.

Clarkson AN, López-Valdés HE, Overman JJ, Charles AC, Brennan KC, Thomas Carmichael S (2013) Multimodal examination of structural and functional remapping in the mouse photothrombotic stroke model. J Cereb Blood Flow Metab 33:716–723.

Coleman ER, Moudgal R, Lang K, Hyacinth HI, Awosika OO, Kissela BM, Feng W (2017) Early rehabilitation after stroke: a narrative review. Curr Atheroscler Rep 19:59.

Conner JM, Chiba AA, Tuszynski MH (2005) The basal forebrain cholinergic system is essential for cortical plasticity and functional recovery following brain injury. Neuron 46:173–179.

Cramer SC, Chopp M (2000) Recovery recapitulates ontogeny. Trends Neurosci 23:265–271.

Dancause N, Barbay S, Frost SB, Plautz EJ, Chen D, Zoubina EV, Stowe AM, Nudo RJ (2005) Extensive cortical rewiring after brain injury. J Neurosci 25:10167–10179.

Farr TD, Whishaw IQ (2002) Quantitative and qualitative impairments in skilled reaching in the mouse (Mus musculus) after a focal motor cortex stroke. Stroke 33:1869–1875.

Fu M, Yu X, Lu J, Zuo Y (2012) Repetitive motor learning induces coordinated formation of clustered dendritic spines in vivo. Nature 483:92–95.

Hofer SB, Mrsic-Flogel TD, Bonhoeffer T, Hübener M (2009) Experience leaves a lasting structural trace in cortical circuits. Nature 457:313–317.

Jones TA (2017) Motor compensation and its effects on neural reorganization after stroke. Nat Rev Neurosci 18:267–280.

Jones TA, Adkins DL (2015) Motor system reorganization after stroke: stimulating and training toward perfection. Physiology (Bethesda) 30:358–370.

Kim SY, Hsu JE, Husbands LC, Kleim JA, Jones TA (2018) Coordinated plasticity of synapses and astrocytes underlies practice-driven functional vicariation in peri-infarct motor cortex. J Neurosci 38:93–107.

Lang KC, Thompson PA, Wolf SL (2013) The EXCITE trial: reacquiring upper-extremity task performance with early versus late delivery of constraint therapy. Neurorehabil Neural Repair 27:654–663.

Mostany R, Portera-Cailliau C (2011) Absence of large-scale dendritic plasticity of layer 5 pyramidal neurons in peri-infarct cortex. J Neurosci 31:1734–1738.

Murphy TH, Corbett D (2009) Plasticity during stroke recovery: from synapse to behaviour. Nat Rev Neurosci 10:861–872.

Nudo RJ (2007) Postinfarct cortical plasticity and behavioral recovery. Stroke 38 [Suppl 2]:840–845.

Nudo RJ, Wise BM, SiFuentes F, Milliken GW (1996) Neural substrates for the effects of rehabilitative training on motor recovery after ischemic infarct. Science 272:1791–1794.

Ramanathan D, Conner JM, Tuszynski MH (2006) A form of motor cortical plasticity that correlates with recovery of function after brain injury. Proc Natl Acad Sci U S A 103:11370–11375.

Roberts TF, Tschida KA, Klein ME, Mooney R (2010) Rapid spine stabilization and synaptic enhancement at the onset of behavioural learning. Nature 463:948–952.

Sullender CT, Mark AE, Clark TA, Esipova TV, Vinogradov SA, Jones TA, Dunn AK (2018) Imaging of cortical oxygen tension and blood flow following targeted photothrombotic stroke. Neurophotonics 5:1.

Tennant KA, Adkins DL, Donlan NA, Asay AL, Thomas N, Kleim JA, Jones TA (2011) The organization of the forelimb representation of the C57BL/6 mouse motor cortex as defined by intracortical microstimulation and cytoarchitecture. Cereb Cortex 21:865–876.

Tennant KA, Kerr AL, Adkins DL, Donlan N, Thomas N, Kleim JA, Jones TA (2015) Age-dependent reorganization of peri-infarct "premotor" cortex with task-specific rehabilitative training in mice. Neurorehabil Neural Repair 29:193–202.

Tennant KA, Taylor SL, White ER, Brown CE (2017) Optogenetic rewiring of thalamocortical circuits to restore function in the stroke injured brain. Nat Commun 8:15879.

Wang L, Conner JM, Nagahara AH, Tuszynski MH (2016) Rehabilitation drives enhancement of neuronal structure in functionally relevant neuronal subsets. Proc Natl Acad Sci U S A 113:2750–2755.

Xu T, Yu X, Perlik AJ, Tobin WF, Zweig JA, Tennant K, Jones T, Zuo Y (2009) Rapid formation and selective stabilization of synapses for enduring motor memories. Nature 462:915–919.

Yang G, Chang PC, Bekker A, Blanck TJ, Gan WB (2011) Transient effects of anesthetics on dendritic spines and filopodia in the living mouse cortex. Anesthesiology 115:718–726.

Yasumatsu N, Matsuzaki M, Miyazaki T, Noguchi J, Kasai H (2008) Principles of long-term dynamics of dendritic spines. Journal of Neuroscience 28:13592–13608.

Yu X, Zuo Y (2011) Spine plasticity in the motor cortex. Curr Opin Neurobiol 21:169–174.

Zeiler SR, Krakauer JW (2013) The interaction between training and plasticity in the poststroke brain. Curr Opin Neurol 26:609–616.